



Experimental Analysis and Energy Balance on Thermal Barrier-Coated Piston Diesel Engine Using Biodiesel

Vidyasagar Reddy Gangula^{1,2} · Govindha Rasu Nandhana Gopal¹ · Hariprasad Tarigonda²

Received: 24 April 2019 / Accepted: 7 August 2020 / Published online: 12 August 2020
© The Institution of Engineers (India) 2020

Abstract In this paper, the effect of the thermal barrier coated (TBC) on top of the piston used in CI engine was investigated when diesel and jatropha biodiesel (JB 100) were used as fuel. Two pistons were selected for TBC coating with a thickness of 50 μ as a bond coat and 250 μ as a topcoat. The first piston was coated with 7% YSZ (LHR 1) and second piston is coated with 2% Nd + YSZ (LHR 2) as a topcoat for the two pistons Ni–Cr–Al–Y used as a bond coat. Experiments were conducted to study the performance, emission and energy balance using standard piston and TBC-coated pistons. The results show that the BTE of an LHR 2 engine using JB 100 is 4.2% higher than the STD diesel engine. The BSFC of an LHR 2 engine using JB 100 fuel was reduced by 11.4% lower than the STD diesel engine. The HC and CO emissions were declined by 20% and 16% for the LHR 2 engine while comparing with the STD diesel engine and NO_x emissions were increased by 15% in the LHR 2 engine with JB 100.

Keywords Nd₂O₃ · Low heat rejection engine · Thermal barrier coatings · YSZ · Jatropha biodiesel

Abbreviations

IC	Internal combustion
TBC	Thermal barrier coating
Nd ₂ O ₃	Neodymium oxide
JB	100 Jatropha biodiesel 100%

LHR	Low heat rejection
BTE	Brake thermal efficiency
STD	Standard engine
CI	Compression ignition
HC	Hydro carbon
CO	Carbon monoxide
NO _x	Nitrogen oxide
EGT	Exhaust gas temperature
YSZ	Yttria-stabilized zirconia
BSFC	Brake specific fuel consumption

Introduction

The present challenges on IC engines are currently focused on reducing engine cost and better fuel consumption, and some technological innovation studies are also conducted [1]. Energy demand is one of most important assessment aspects for the IC engine. In particular, from the thermodynamics second law, it states that total input energy is not possible to transform into useful work. In other words, 100% efficiency can never be achieved due to some amount of heat rejection in the exhaust gases, heat loss due to coolant and unaccounted losses. In this connection, ceramic coating in IC engine is one of the promising alternatives. Ceramic coatings act as an insulator to resist the heat transfer from cylinder to the engine cooling system. Researchers are mainly focusing on removing the cooling system in the IC engines. In this way, the cost and weight of the engine will decrease, and higher efficiency can be achieved [2].

The LHR ideas have gained attention through the 1980s, when a wide range of researchers studied the “semi-

✉ Hariprasad Tarigonda
thprasads@gmail.com

¹ School of Mechanical Engineering, VIT University, Vellore 632 014, Tamilnadu, India

² Sree Vidyanikethan Engineering College, Tirupathi 517102, Tamilnadu, India

adiabatic engine.” The researchers focus on improving engine efficiency by partially/completely suppressing energy loss due to the combustion chamber walls. LHR engine designs have been comprehensively adopted by thermal barrier coatings (TBC’s) [3]. TBC applied to combustion chambers for diesel engines are intended to lower heat through the inside cylinder to the engine cooling system. Figure 1 shows that useful energy is increased from 32 to 36%, exhaust energy is increased from 28 to 35%, and coolant energy is decreased from 26 to 19% due to ceramic coating [2].

Studies showed that engine insulation would remove the necessity for such a coolant system and increases the exhaust gas energy density, enabling them to recover a significant proportion of that energy and thus the overall efficiency gain of up to 10% [4]. The internal combustion engine isolated by thermal barrier coating materials among its cylindrical head, walls, piston, valves, etc., known as LHR engines. Due to the addition of TBC materials, major promises of LHR engines represent a significant increase in thermal efficiency, reduced emissions and reduced fuel economy and the imposition of the method of cooling from the engine [5].

Numerous ceramic coatings have adopted in engine development [6]. Based on the literature, inside, the engine coated with various low thermal conductivity TBC materials such as PSZ [7], $\text{Al}_2\text{O}_3\text{--TiO}_2$ [8] and YSZ [9]. Partially stabilized zirconia (PSZ), is mostly 6–9% of YSZ, is the most used ceramic material composition, and it exhibited better performance in higher temperatures [10]. The authors clearly showed that related to the STD engine, the LHR engine BTE was increased and marginally reduced by BSFC. Further, a decrease in coolant heat exchange has been shown to increase exhaust heat by nearly 15–25%. The emissions of CO and HC in the TBC engine are decreasing [11]. Major research in the TBC engine has shown that thermal efficiency has been improved individually by 14% and 7% for completely adiabatic and semi-adiabatic conditions [12]. Few

researchers presented that the LHR engine with a thickness of 0.1-mm YSZ on the head of the cylinder, piston and liner covered with a thickness of 0.5 mm YSZ enhanced brake specific fuel consumption by 4–5% at all loads [13]. However, many investigators showed that the TBC engine increases the NOx emission levels [14]. Several tests have been conducted to detect the effects of biodiesel and semi-adiabatic IC engines, out of this, LHR engines using biodiesels are also found to considerably improve the efficiency of LHR engines [15].

In the study of ZrO_2 coated in CI engine with cotton seed blends (B15, B35 and B65), it is reported that an increase in output power for the ceramic coated diesel and reduced emissions with coated biodiesel operation [16]. Several studies have shown that the LHR engine using biofuel and its blends prepared from cashew nutshell reduces BTE and emission levels compared with the STD engine [17]. The mahua biodiesel CI engine showed higher performance and better emission controls compared to diesel fuel [18].

The main characteristic of TBC materials is thermal conductivity. The literature shows that the main drawback of 7% YSZ is over 1200 °C, changing the unfavorable stage changes, due to stage changes that direct to crack development in the top surface. Modern improvements in defining a substitute for YSZ topcoat found numerous innovative ceramics having better advantages at temperatures above 1200 °C [19]. For example, rare-earth oxides like Gd_2O_3 , Yb_2O_3 and Nd_2O_3 have reported that they are much less thermal conductivity than YSZ. Thermal conductivity was reduced by adding two or more oxides to zirconia. Combined dopants may lessen the thermal conductivity by around 15–30% while comparing with YSZ ceramics and get better the sintering stability of the TBC coating at maximum temperatures [20–22]. Recent trends to determine on the effect of three different doping rare-earth oxides into YSZ composition with thickness of 0.25 mm. The outcomes of the reveals that in ceramic engine, HC and CO emissions were decreased marginally

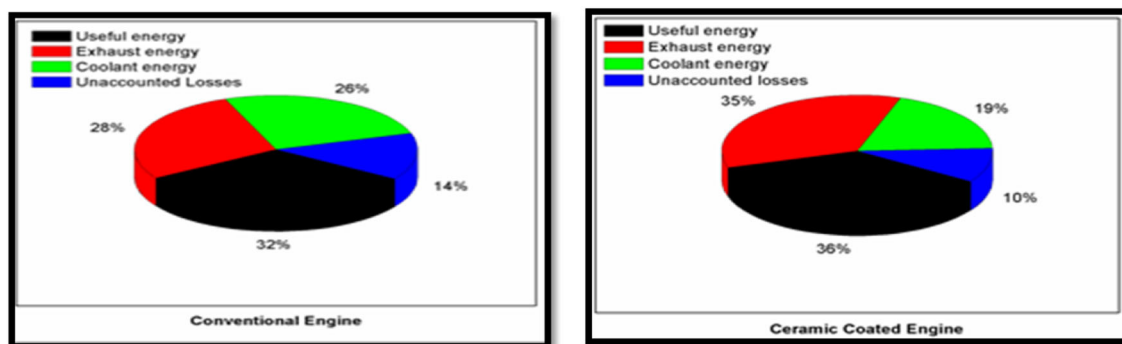


Fig. 1 Comparison of energy distribution between conventional and ceramic-coated engines [2]

and a major growth of NO_x emission when compare to STD fuel engine [23].

From the referred literatures, it has been observed that performance and emission features of CI engine can be optimized by using biodiesels with ceramic coatings. Only limited papers were presented in the different biodiesels with semi-adiabatic type engines like LHR engines. In this present work, experiments were performed on CI engine by using diesel and jatroptha fuels, and the piston crown was covered in two different combinations of pistons by 250 μ of thickness like 7% YSZ (LHR 1), 2% Nd–YSZ (LHR 2) by using plasma spray method.

Testing Materials and Methods

Test Fuels

The tested fuel adopted in the study was diesel fuel and jatroptha biodiesel (JB 100). The diesel and Jatroptha properties were obtained using ASTM D6751 standards presented in Table 1.

Preparation of LHR Engine

In this exploration analysis, plasma spray system is used for the coating. This process involved in three stages such as preparation of piston crown surface, bond coating and top ceramic TBC layer. Figure 2 shows the plasma spray coating system. The thermal barrier of piston consists of two different interfaces; they are piston top substrate to bond coat and bond coat to top ceramic layer. In the present study, the coating is performed on the aluminum alloy piston substrate. The noted specifications of plasma spray system are revealed in Table 2.

The coating procedure is: first, a 0.3-mm thickness of the piston crown surface was removed by the machining process before coating. The quantity of piston surface material separated by the lathe machining process should be the same to the volume of TBC added to the piston. After completing the process, the piston top surface was first covered with a Ni–Cr–Al–Y bond coat with thickness of 50 μ and same coat applied on two different pistons. The

Table 1 Properties of test fuels

Properties	Diesel	Jatroptha (JB 100)
Kinematics viscosity at 40 °C (cst)	2.75	4.85
Density at 15 °C (kg/m ³)	845	866
Flash point (°C)	65	162
Fire point (°C)	73	169
Calorific value (MJ/kg)	42	39

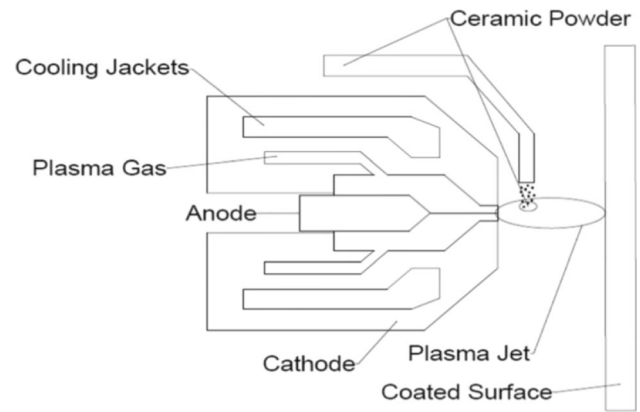


Fig. 2 Plasma spray coating system

Table 2 Specifications of plasma spray method

Coating variables	Details
Plasma gun	3 MB plasma spray gun
Flow rate of hydrogen gas	16–19 LPM
Pressure of organ gas	100–120 PSI
Spraying distance	3–4 in.
Nozzle	GH type nozzle
Flow rate of organ gas	81–91 LPM
Pressure of hydrogen gas	50 PSI
Powder feed rate	40–46 g/min

topcoat layer of two different pistons comprises a 250-μ thickness. The top ceramic coat materials are 7% YSZ and 2% Nd + YSZ coating through the plasma spray gun, this coating combination replaces the actual piston dimensions. The composition of coating materials is shown in Table 3. The schematic setup of TBC system is depicted in Fig. 3.

Experimental Test Setup

The Kirloskar engine used for the experimental studies, 4 stroke, 1-cylinder, water cooled, vertical and direct injection C.I engine with, ratio of compression as 17.5:1, evolving 5.2 kW at rated speed of 1500 rpm has been adopted for this present exploration. The experiment was performed at various loads using diesel and JB 100 fuels with and without ceramic coatings. A dynamometer is employed for loading point with steady speed at 1500 rpm. A piezoelectric pressure transducer located at the cylinder head is used for assessing in-cylinder pressure. Chromel–Alumel thermocouples have been placed in the outlet pipe for measuring EGT. Fuel flow has been assessed by using a 50 cc graduated burette and stopwatch. The AVL DI GAS 444-5 gas analyzer was adopted for measurement of NO_x, CO and HC emissions of the tail pipe [24]. The schematic

Table 3 Details of the coating material and the compositions used

TBC layers	Coating material	Composition	Thickness	Particle size
Bond coat	NiCrAlY	(67% Ni, 22% Cr, 10% Al, 1% Y)	50	56–106
Topcoat	7YSZ	(7% Y, 93% ZrO ₂)	250	56–106
	2 mol% Nd-YSZ	(2% Nd ₂ O ₃ + 5% Y + ZrO ₂)	250	56–106

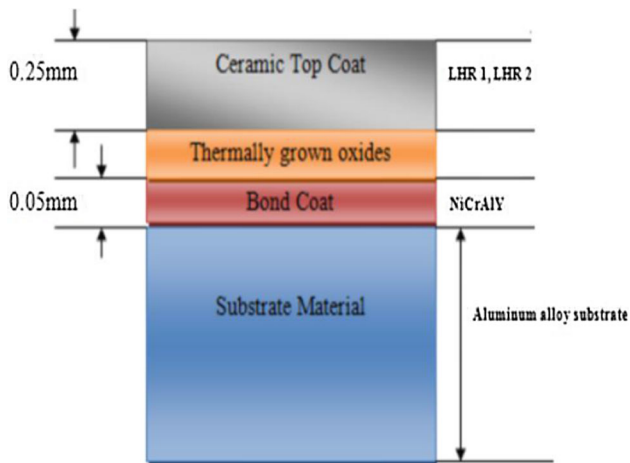


Fig. 3 Schematic of TBC system showing each layer and its material of test engine setup is exhibited in Fig. 4. The snapshot of engine setup and coated piston arrangement are displayed in Fig. 5.

The fuel economy, exhaust emissions and exhaust gas temperature have been quantified and verified for different loads. The STD engine was tested to determine the engine's performance and pollution characteristics with diesel and jatropha fuel at vastly different loads. The same

method was repeated with diesel and jatropha fuels on the coated engines. The engine speed has been kept constant throughout the engine procedure at 1500 rpm. The results were finally compared. However, every test has been conducted repeatedly thrice to further check output and engine exhaust data. The mean of values is used for any further graphical analysis and inclusion. The snapshots of TBC-coated piston and STD piston are presented in Fig. 6. The complete information of the different engine tests is exhibited in Table 4. The test engine parameter is seen in Table 5.

Thermal Analysis

Steady-state thermal analyses were performed to analyze the impact of the TBC on the CI engine of different ceramic-coated pistons. The temperature contrasts on the piston crowns are examined for both coated and uncoated pistons are discussed steadily. The generic package software ANSYS was used to conduct thermal analyses. It is well reported that heat transfer mechanisms are specific in the CI engine piston surface. The primary heat transfer between the combustion chamber and the piston top surface is often assumed to be convection in the thermal

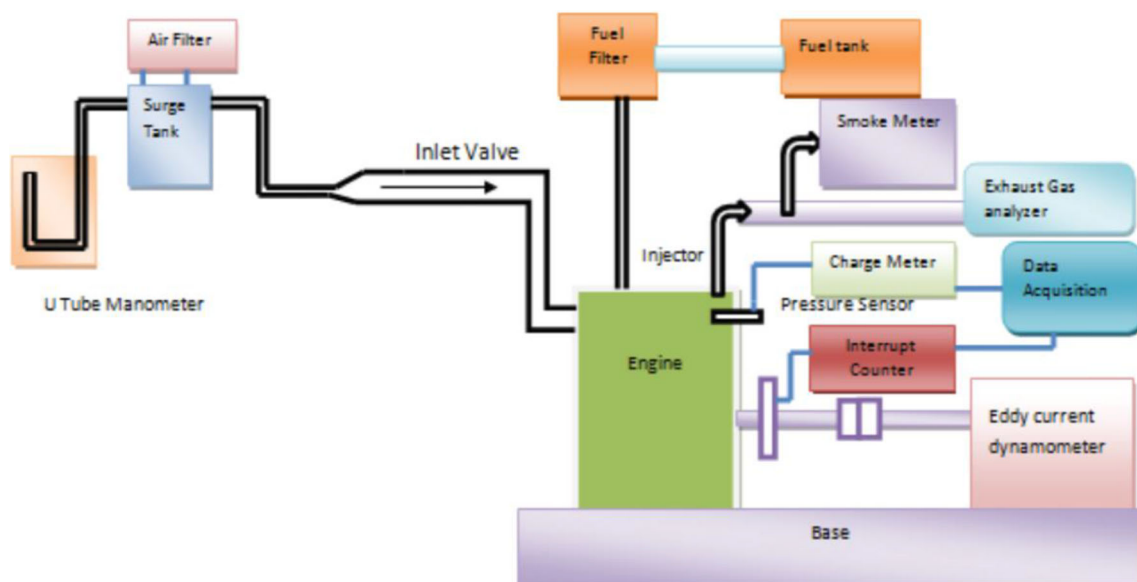


Fig. 4 Schematic arrangement of experimental setup

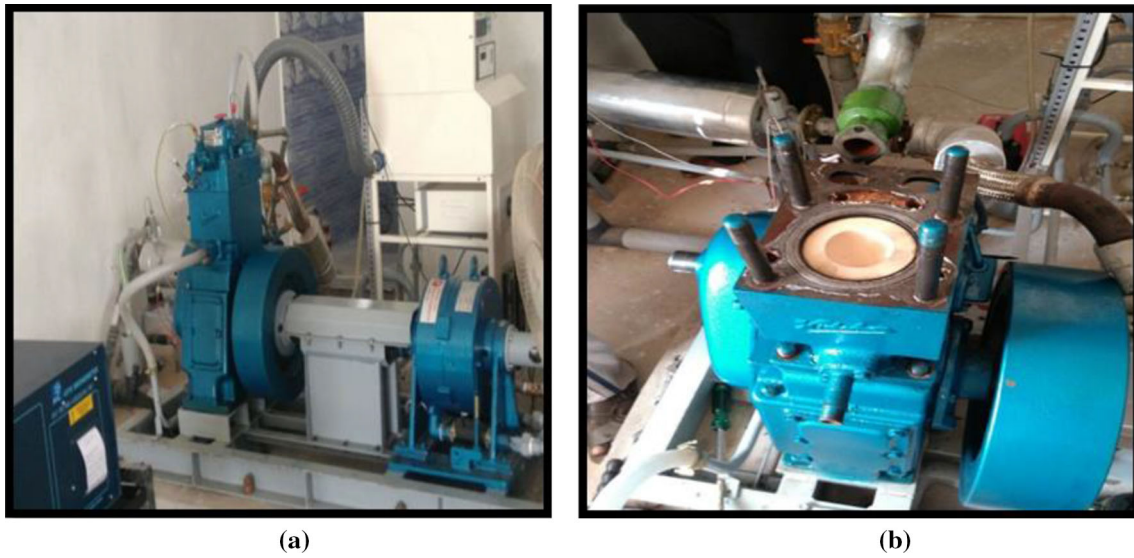


Fig. 5 Snapshots of **a** engine setup and **b** coated piston arrangement

Fig. 6 Snapshots of **a** uncoated STD engine piston and **b** coated piston

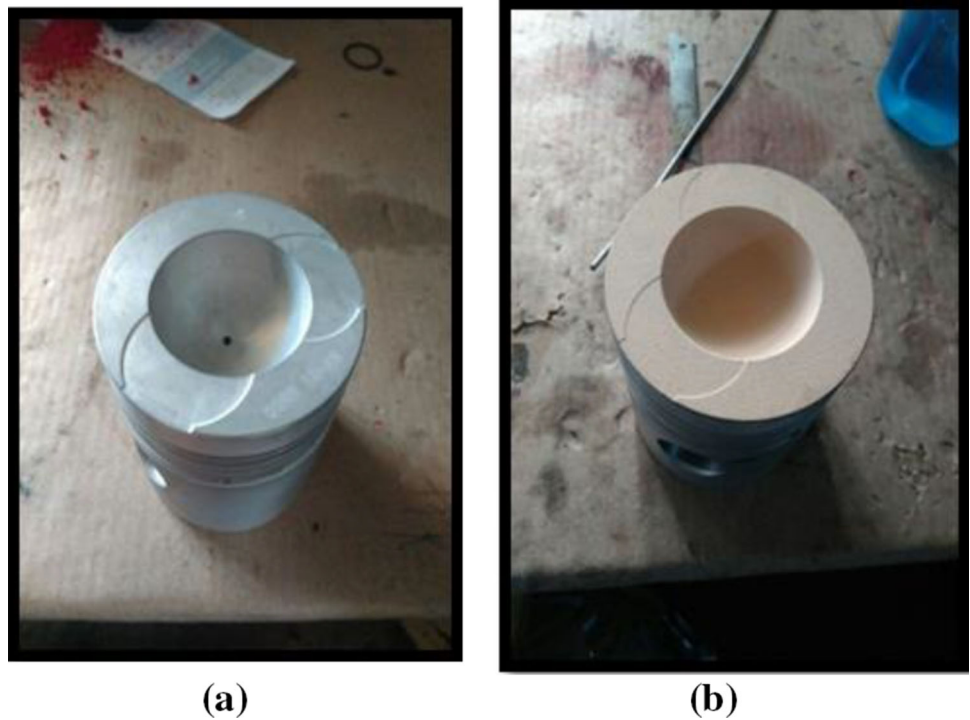


Table 4 Details of the four different engine tests

Testing condition	Type of engine
Uncoated diesel fuel	Standard engine (STD)
Uncoated jatropha biodiesel (JB 100)	Standard engine (STD)
7% Y + 93% ZrO ₂ (JB 100)	LHR 1
2% Nd ₂ O ₃ + 5% Y + 93% ZrO ₂ (JB 100)	LHR 2

analyses [25]. A convection heat charge with the effect of radiation is applied to the surface of the piston crown. That is, the convection heat charge is increased to take radiation effect into account. Local average heat transfer coefficient and gas temperature limit conditions are calculated by using the simulation code for the piston surface [25–27]. The code determines the heat transfer coefficients at a period of one crank angle degree. The following equation

Table 5 Specifications of test engine

Type	Specifications
Engine	4-Stroke, single cylinder water-cooled diesel engine
Rated speed	1500 rpm
Loading	Electric loading
Stroke	110 mm
Orifice diameter	29.6 mm
Compression ratio	17.5:1
Bore diameter	87.5 mm
Compression ratio	17.5:1

developed by Hohenberg [28] is used in the experiments to determine rapid heat transfer coefficients (HTC).

$$h_{\text{gas}}(t) = \alpha V_c(t)^{-0.06} P(t)^{0.8} T(t)^{-0.4} (S_p + b)^{0.8} \quad (1)$$

where $h_{\text{gas}}(t)$ is the convective HTC ($\text{W}/\text{m}^2 \text{K}$), $V_c(t)$, $P(t)$ and $T(t)$ are the cylinder volume (m^3), pressure (bar) and temperature (K), and S_p the mean piston speed (m/s). The calibration parameters a and b are measured as 130 and 1.4. The mean time values of HTC and temperature are often used for the piston top. From the literature, the boundary conditions from the oil-cooled portion of the piston are as 95°C and $1500 \text{ W}/\text{m}^2 \text{C}$ [27]. The other limited boundary conditions (temperature HTC) are considered from the advanced literature shown in Fig. 7 [25, 26].

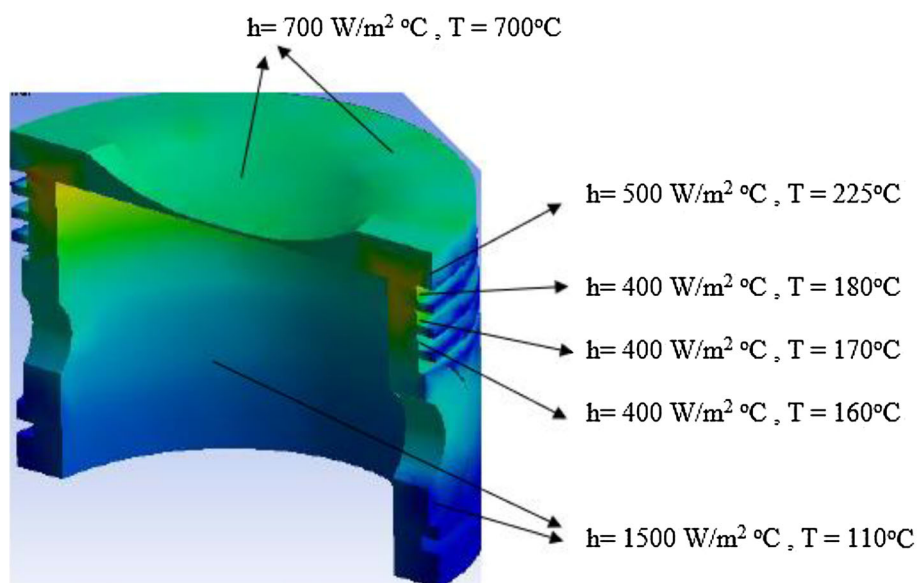
A counterplot of the temperature is presented in Fig. 8 for the uncoated piston. In the crown center and the bowl lip regions, the high temperatures are predicted since the

heat flux is subject to the circumference. Highest temperature falls at the middle of the piston surface, and the piston bowl edges and least temperature are at the piston base. Highest and least temperature values are reached at around 299.13°C and 158.02°C , respectively, for uncoated pistons. The temperature falls radial from the center of the crown to the bowl, and then it increases toward the lips of the bowl and indeed decreases again on the corner of the surface of the head.

Under similar circumstances, counterplots of the temperature allocation are illustrated in Fig. 8 for the different ceramic-coated pistons such as LHR (1 and 2). The figure showed that only temperature values are altered, but that there are no changes in counterplots. It is observed that the maximum values of ceramic-coated pistons are 645.9°C and 646.03°C and minimum are 187.61°C and 187.67°C , respectively. In comparison with the top-surface-uncoated piston temperature, 53.68% and 53.69% have been raised.

The coated pistons have a maximum temperature than the STD piston because of its thermal property. From this study, the top surface temperature of the piston has increased, and the surface temperature of the substrate has decreased. When investigating the radial dispersion of the temperature, the piston temperature drops from the center of the crown to the bottom of the bowl and then decreases at the edge of the crown again after the increase toward the lips of the bowl. This happens because the flame propagation lowers due to the cooling near the cylinders. The maximum temperature enhances engine performance by increased fuel consumption and reducing emissions of hydrocarbon.

Fig. 7 Thermal boundary conditions of the used piston [25]



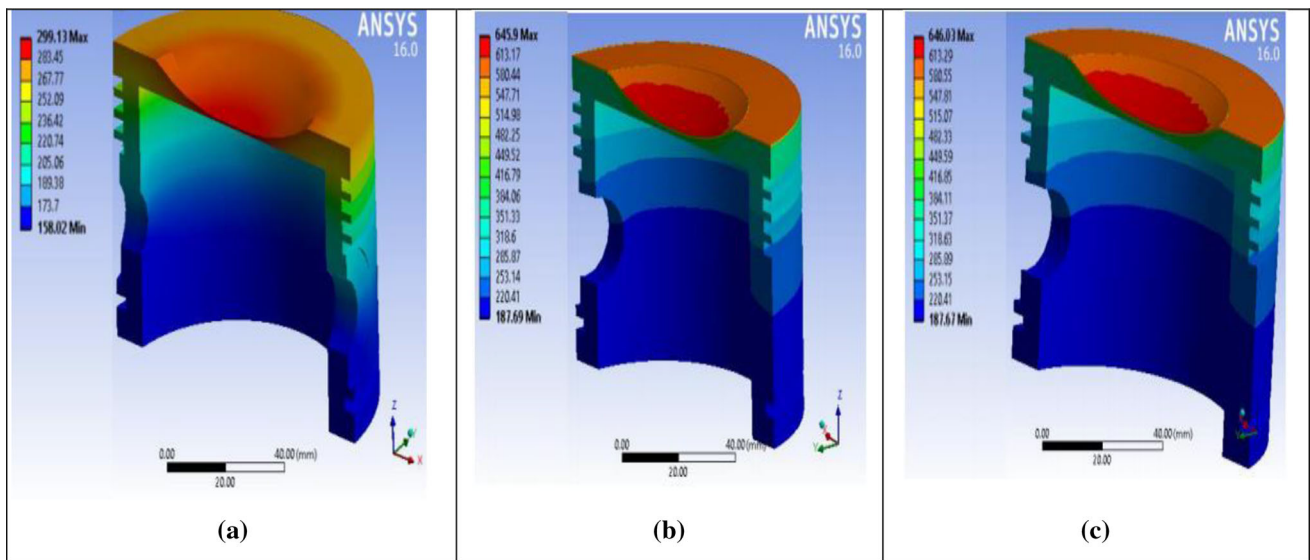


Fig. 8 Temperature distribution of a STD engine, b LHR 1 engine and c LHR 2 engine

Results and Discussion

Brake Thermal Efficiency (BTE)

The variation of BTE with BP is presented in Fig. 9 for both the STD- and TBC-coated engines LHR (1 and 2). The experimentation outcome exhibits that the BTE for STD engines using diesel and JB 100 fuel, LHR (1 and 2) engines using JB 100 are found to be 30.6%, 28.7%, 31.42% and 31.96%. The LHR (1 and 2) engines' BTE is increased by 2.6% and 4.2%, respectively, while comparing with STD engine using diesel fuel. The maximum BTE was found by LHR 2 engine using JB 100. This may be due to adding of low thermal conductivity doping agent into ceramic material composition, which it increases the

thermal resistance on the top of the piston, and this resistant heat further enhances the efficiency [20, 29]. The addition of TBC coating and more oxygen buffers in the JB 100 leads to higher thermal efficiency [30, 31].

Brake Specific Fuel Consumption (BSFC)

The deviation of BSFC with BP is presented in Fig. 10 for both the STD- and TBC-coated engines LHR (1 and 2). It is noted that LHR (1 and 2) engines shows minimum BSFC values when compared with STD diesel fuel engine. The reduction in BSFC was found to be 10.5% and 11.4%, respectively, when compared to STD engine. The BSFC is reciprocal of BTE so that all LHR engines gives better BSFC reduction when compare to STD engine. This can be

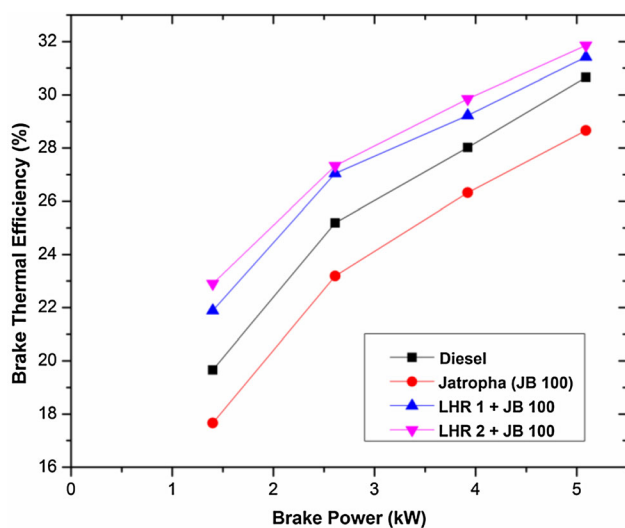


Fig. 9 Brake thermal efficiency versus brake power

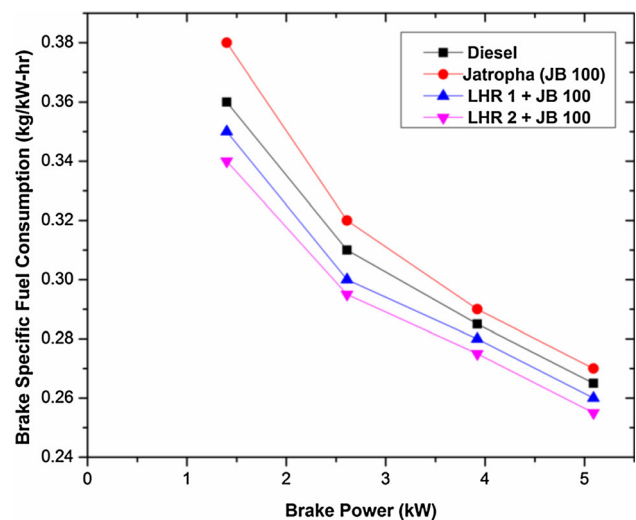


Fig. 10 Brake specific fuel consumption versus brake power

caused by the addition of low thermal conductivity dopants into the TBC system of the LHR engine; the more heat resistant it increases the cylinder temperature, which increases the fuel temperature in the combustion chamber [32].

Variation of Cylinder Pressure (CP)

The deviation of CP with crank angle is presented in Fig. 11 for both the STD- and TBC-coated engines LHR (1 and 2). The peak cylinder pressure was attained by LHR (1 and 2) engines when compared to the STD engine. The increase in the pressure of cylinder has been observed to be 5% and 6.7%, respectively, compare to STD engine using diesel fuel. The LHR engines led to increased peak pressure within the combustion chamber. In the preliminary mixed stage, more fuel could be consumed which leads to higher heat generated for TBC engines [7].

Variation of Heat Release Rate (HRR)

The deviation of HRR with crank angle is presented in Fig. 12 for both the STD- and TBC-coated engines LHR (1 and 2). The maximum HRR was obtained by LHR (1 and 2) engines when compared to the STD diesel fuel engine. The increase in the HRR of LHR engines was found to be 6.7% and 10.6%, respectively, compare to STD engine using diesel fuel. The cause for getting increased HRR is because of adding thermal protection in the piston crown that has the tendency of higher HRR in LHR engines [33].

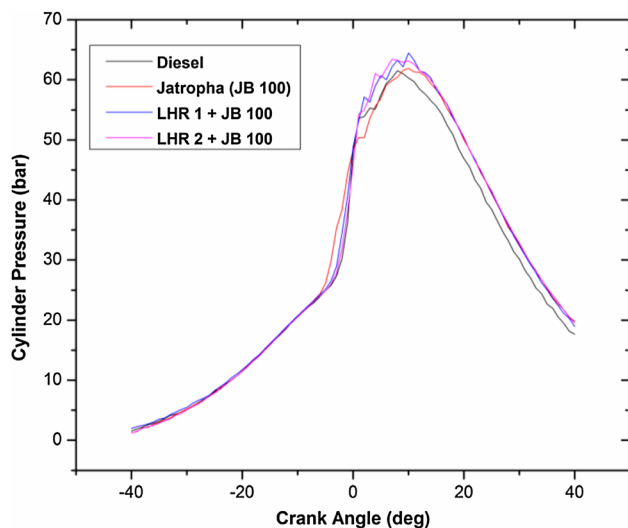


Fig. 11 Cylinder pressure versus crank angle

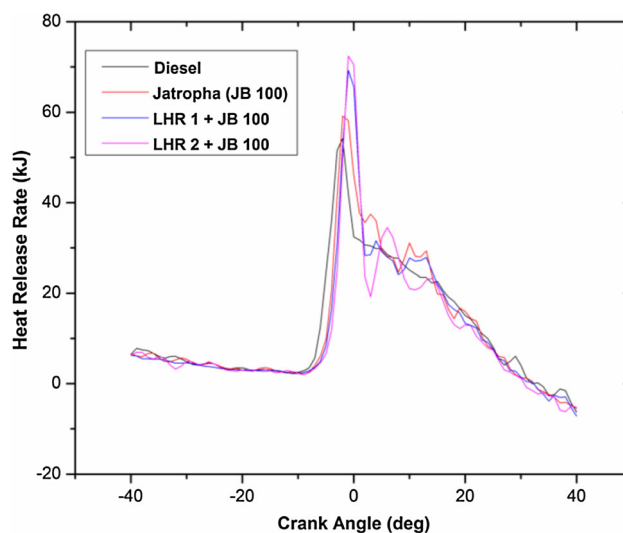


Fig. 12 Heat release rate versus crank angle

Exhaust Gas Temperature (EGT)

The variation of EGT with BP is presented in Fig. 13 for both the STD- and TBC-coated engines LHR (1 and 2). The results showed that the EGT for STD engine with diesel fuel and JB 100 was 290 °C and 298 °C, while LHR engines with JB 100 fuel were 315 °C and 320 °C, respectively. It confirms that LHR engines show the maximum EGT than the STD engine. The increase in EGT was found to be 7.9% and 9.3% comparing to the STD engine using diesel fuel. This is because EGT is related to more heat in the engine cylinder, which leads to an increased temperature of combustion [34].

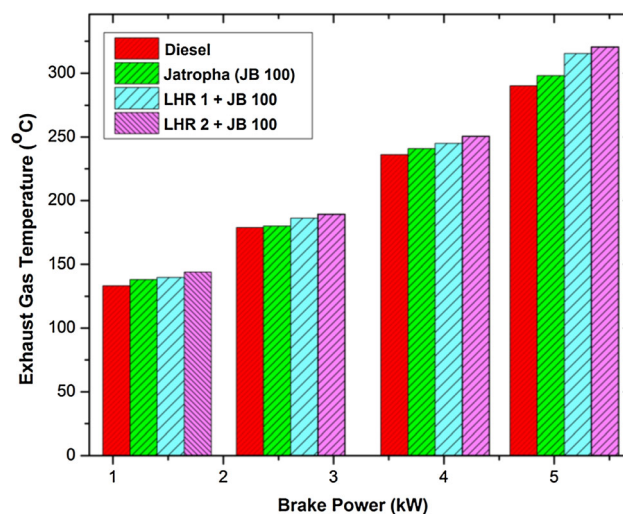


Fig. 13 Exhaust gas temperatures versus brake power

Energy Balance

Figure 14 shows the energy balance of the STD engine using diesel and JB 100 fuel, TBC-coated engines LHR (1 and 2) using JB 100 fuel.

Loss of Energy from Exhaust Gases

Hot exhaust gases carry a key part of the fuel contribution energy [35]. At high load conditions, energy increased by the exhaust gas in LHR (1 and 2) engines by 13% and 14.9% when compare to STD engine using diesel fuel. This is because of fuel consumption in the TBC engine is decreased at greater loads and significantly increased at lesser loads. The available heat at the outlet is greatly augmented in all loading conditions due to ceramic coating.

Engine Cooling Energy Losses

Adding ceramic coatings to the piston head, it reduces the heat transfer from the coolant. At higher load conditions, cooling energy losses are decreased for LHR (1 and 2) engines by 15% and 17.4% when compare to STD engine using diesel fuel.

Useful Energy

Due to the ceramic coating, the heat rejected to the LHR engines is reduced to more. As a result, the BTE was marginally improved by low thermal loss. At high load conditions, in the LHR engine, useful energy increased by 1.7% and 3.5% when compare to the STD engine using diesel fuel.

Unaccounted Losses

Unaccounted losses mainly occur due to environmental heat loss, such as conduction, convection and radiation, the heat exchange from outside engine surfaces to the surrounding areas. At high load conditions, in the LHR 2 engine, unaccounted losses decreased by 2.5% when compared to the STD engine using diesel fuel.

Hydrocarbon Emissions (HC)

The deviation of HC with BP is presented in Fig. 15 for both the STD- and TBC-coated engine LHR (1 and 2). It confirms that LHR engines have lower HC emissions than STD diesel fuel engine. The results showed that HC emissions in the LHR (1 and 2) TBC engines decreased

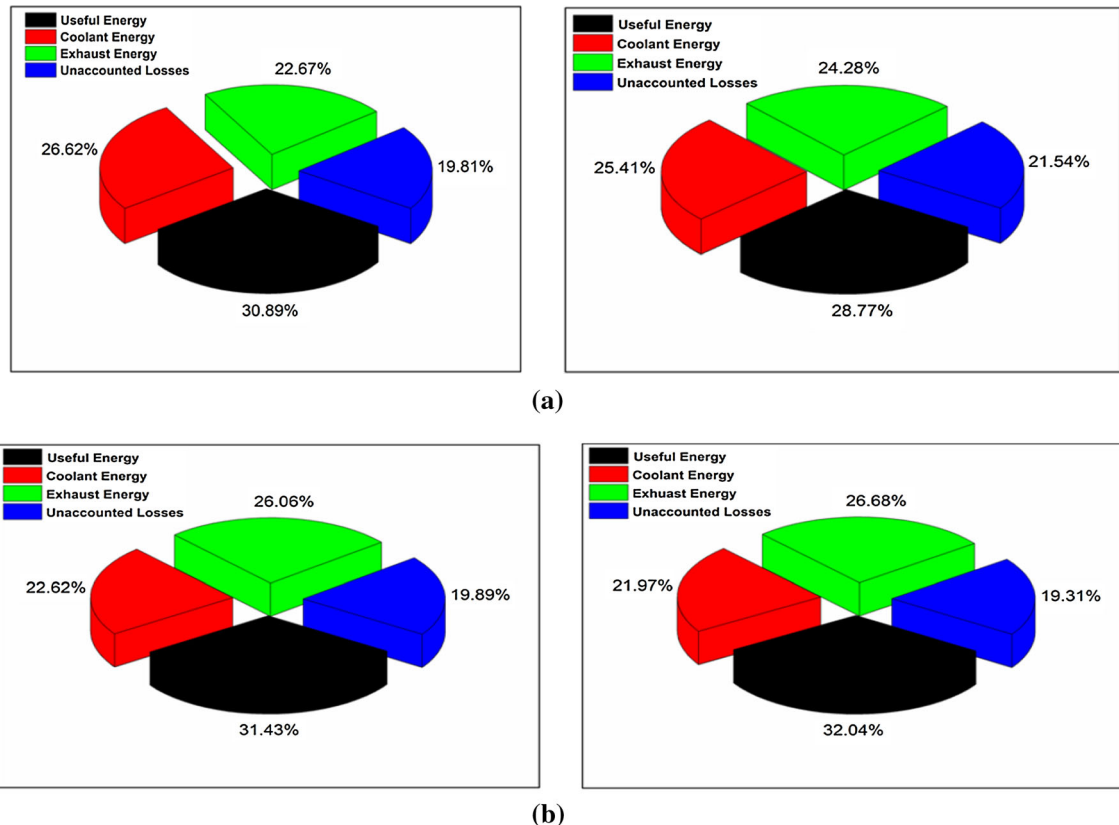


Fig. 14 a Variation in energy distribution of standard engines using diesel and jatropha (JB 100). b Variation in energy distribution of coated engines LHR 1 and LHR 2 using jatropha (JB 100)

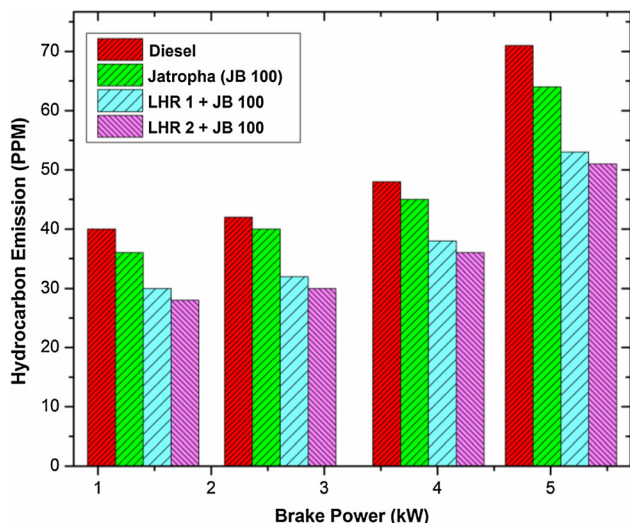


Fig. 15 Hydrocarbon emission versus brake power

from 17.1 to 20.3% compared to the STD engine using diesel fuel. This is because of an increase in the temperature of combustion chamber in TBC engines which results in the burning of the hydrocarbon in the fuel and reduces the unburned hydrocarbon emissions. Previous researchers have reported that HC emissions in LHR engines using biodiesels have been reduced because of more oxygen in biodiesels results in complete and proper combustion [36].

Carbon Monoxide Emission (CO)

The variation of CO with BP is presented in Fig. 16 for both the STD- and TBC-coated engines LHR (1 and 2). It indicates that LHR engines have lower CO emissions than STD diesel fuel engine. The results showed that CO emissions in the LHR (1 and 2) TBC engines decreased

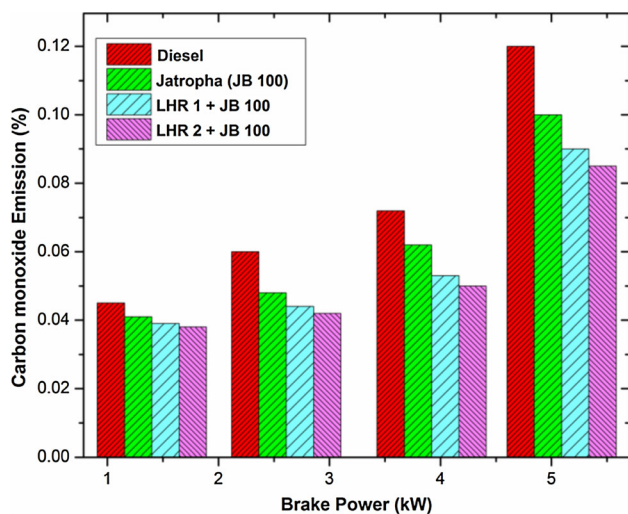


Fig. 16 Carbon monoxide emission versus brake power

from 14 to 16%, respectively, when compared to the STD engine. This is due to ceramic coating the improved combustion of the fuel due to more quantity of heat present in the combustion chamber. In coated engines, the addition of TBC coating and extra oxygen content in the JB 100 leads to better combustion and reduces CO emissions [37].

Nitrogen Oxide Emission

The variation of NO_x with BP is presented in Fig. 17 for both the STD- and TBC-coated engines LHR (1 and 2). It indicates that LHR engines have higher emissions of NO_x compared to STD engines with full load. The results showed that NO_x emissions in the LHR (1 and 2) TBC engines increased from 12 to 15%, respectively, compared to the STD diesel fuel engine. This is due to increased interaction between O_2 and N_2 at high combustion temperatures in the LHR engines and therefore increased NO_x emissions. The biodiesels give very high NO_x emission due to the higher in-cylinder combustion temperature in LHR engines and oxygen contented in the biodiesel increases NO_x emission [29, 38].

Smoke Opacity

The variation of smoke opacity with BP is presented in Fig. 18 for both the STD- and TBC-coated LHR (1 and 2) engines. It shows that the smoke opacity of LHR engines is lower than the STD engine. The results clearly indicate that the LHR 2 engine decrease in smoke opacity by 14.1% when compared to STD engine using JB 100 fuel. This happens because of proper ignition and better air–fuel mixture in LHR engines are responsible for reduction in smoke emission. Previous researchers noted the coating in

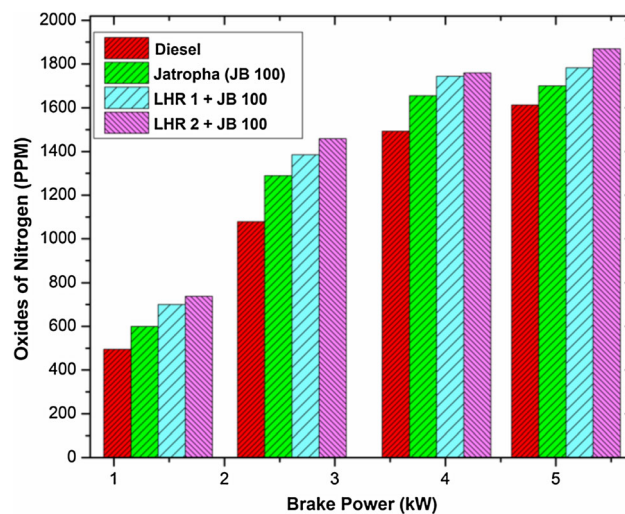


Fig. 17 Oxides of nitrogen versus brake power

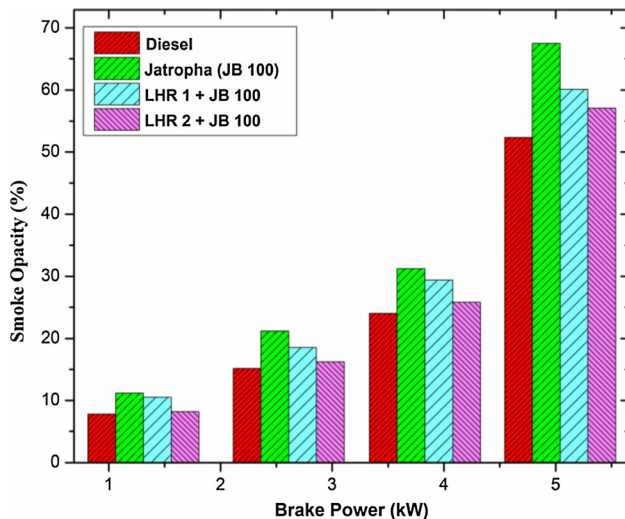


Fig. 18 Smoke opacity versus brake power

the combustion chamber increases the gas temperature and that the opacity of smoke decreases significantly with the LHR engine [7].

Conclusion

The standard CI engine was transformed into an LHR engine by wrapping its piston surface with a 250- μ coating thickness of two different TBC pistons like LHR (1 and 2) by plasma spray method. Engine variables like BTE, BSFC, EGT and emissions like HC, CO, Smoke and NO_x are measured in this investigation. The following are the specific conclusions for optimized conditions of the engine to obtain maximum efficiency and lower emissions

- For maximum BTE and lower BSFC, the engine should be operated with LHR 2 engine using JB 100 fuel.
- For maximum EGT, the engine should be operated with LHR 2 engine using JB 100 as a fuel.
- For peak pressure and maximum HRR, the engine should be operated with LHR 2 engine using JB 100 fuel.
- For lower emissions of HC and CO, the engine should be operated with LHR 2 engine using JB 100 as a fuel.
- For lower NO_x emission, the engine should be operated with STD engine using diesel fuel.
- For lower smoke opacity, the engine should be operated with LHR 2 engine using JB 100 fuel.
- By using insulation to reduce heat loss in the engine cooling system, the cylindrical walls are warmer, and the gas exhaust energy is increased. In comparison with the standard engine (without coating), the heat loss in the exhaust for high, medium and low load in LHRE is increased.

References

1. R. Prasad, V.R. Bella, A review on diesel soot emission, its effect and control. *Bull. Chem. React. Eng. Catal.* **5**, 69–86 (2011)
2. R. Kamo, W. Bryzik, Adiabatic Turbocompound Engine Performance Prediction. SAE (Soc. Automat. Eng.) Paper 780068, 1978
3. M. Bailey, Comparative evaluation of three alternative power cycles for waste heat recovery from the exhaust of adiabatic diesel engines. NASA Tech. Memo 86953, 1985
4. F.J. Wallace, T.K. Kao, M. Tarabad, W.D. Alexander, A. Cole, Thermally insulated diesel engines. *Proc. Inst. Mech. Eng.* **198A**(5), 97–105 (1984)
5. E. Buyukkaya, M. Cerit, Experimental study of NO_x emissions and injection timing of a low heat rejection diesel engine. *Int. J. Therm. Sci.* **47**, 1096–1106 (2008)
6. X. Cao, R. Vassen, D. Stoeber, Ceramic materials for thermal barrier coatings. *J. Eur. Ceram. Soc.* **24**, 1–10 (2004)
7. B.R. Prasath, P. Tamilporai, M.F. Shabir, Analysis of combustion, performance and emission characteristics of low heat rejection engine using biodiesel. *Int. J. Therm. Sci.* **49**, 2483–2490 (2010)
8. H. Hazar, U. Ozturk, The effects of Al₂O₃–TiO₂ coating in a diesel engine on performance and emission of corn oil methyl ester. *Renew. Energy* **35**, 2211–2216 (2010)
9. C. Haşimoğlu, M. Ciniviz, I. Özsert, Y. İçingür, A. Parlak, M.S. Salman, Performance characteristics of a low heat rejection diesel engine operating with biodiesel. *Renew. Energy* **33**, 1709–1715 (2008)
10. C. Lima, R. Trevisan, Temperature measurements and adhesion properties of plasma sprayed thermal barrier coatings. *J. Therm. Spray Technol.* **8**, 323–327 (1999)
11. J. Muthusamy et al., Experimental investigation of thermal barrier (8YSZ–TiO₂–Al₂O₃) coated piston used in direct injection compression ignition engine. *Therm. Sci.* **20**(4), S1189–S1196 (2016)
12. F.J. Wallace, R.J.B. Way, H. Vollmert, et al. Effect of partial suppression of heat loss to the coolant on the high output diesel engine cycle. SAE Paper No. 790823, 1979
13. P.H. Havstad, I.J. Gervin, W.R. Wade, A ceramic insert uncooled diesel engine, SAE Paper No. 860447, 1986
14. N. Panneerselvam, A. Murugesan, C. Vijayakumar, A. Kumaravel, D. Subramaniam, A. Avinashd, Effects of injection timing on bio-diesel fuelled engine characteristics—an overview. *Renew. Sustain. Energy Rev.* (2015). <https://doi.org/10.1016/j.rser.2015.04.15>
15. B. Deepanraj, G. Sankaranarayanan, P. Lawrence, Performance and emission characteristics of a diesel engine fueled with rice bran oil methyl ester blends. *Daffodil Int. Univ. J. Sci. Technol.* **7**(2), 51–55 (2012)
16. H. Hazar, Characterization and effect of using cotton methyl ester as fuel in a LHR diesel engine. *Energy Convers. Manag.* **52**, 258–263 (2011)
17. S. Santhanakrishnan, B.K.M. Ramani, Performance emission and combustion characteristics of a low heat rejection engine fuelled with diesel-CNSO-EEA blend. *J. Adv. Eng. Res.* **2**, 29–33 (2015)
18. P. Sukumar, G. Nagarajan, N. Vedaraman, B.V. Ramabramham, Mahua oil (*Madhuca indica* oil) derivatives as a renewable fuel for diesel engine systems in India: a performance and emissions comparative study. *Int. J. Green Energy* **4**, 89–104 (2007)
19. P.N. Shirao, A.N. Pawar, An overview on thermal barrier coating (TBC) materials and its effect on engine performance and emission. *Int. Rev. Mech. Eng.* **5**(5), 973 (2011)

20. S. Raghavan, H. Wang, W.D. Porter, R.B. Dinwiddie, M.J. Mayo, Thermal properties of zirconia co-doped with trivalent and pentavalent oxides. *Acta Mater.* **49**, 169–179 (2001)
21. D. Zhu, R.A. Miller, Thermal conductivity and sintering behavior of advanced thermal barrier coatings. NASA, TM-211481, 2002
22. J.R. Nicholls, K.J. Lawson, A. Johnstone, D.S. Rickerby, Methods to reduce the thermal conductivity of EB-PVD TBC's. *Surf. Coat. Technol.* **151–152**, 383–391 (2002)
23. G. Vidyasagar Reddy, N. Govindha Rasu, T. Hari Prasad, Analysis of performance and emission characteristics of TBC coated low heat rejection engine. *Int. J. Ambient Energy* (2019). <https://doi.org/10.1080/01430750.2019.1567581>
24. U. Rashmi, Indian Emission Regulations. The Automotive Research Association of India, Booklet. https://www.araaiindia.com/pdf/Indian_Emission_Regulation_Booklet.pdf. SAE Paper No. 890142A, 2017
25. E. Buyukkaya, Thermal analysis of functionally graded coating AlSi alloy and steel pistons. *Surf. Coat. Technol.* **202**, 3856–3865 (2008)
26. E. Buyukkaya, M. Cerit, Thermal analysis of a ceramic coating diesel engine piston using 3D finite element method. *Surf. Coat. Technol.* **202**, 398–402 (2007)
27. J.G. Muchai, A.D. Kelkar, D.E. Klett, J. Sankar, Thermal–mechanical effects of ceramic thermal barrier coatings on diesel engine piston. *Mat. Res. Soc. Symp. Proc.* **697**, 10–16 (2002)
28. G.F. Hohenberg, Advanced approaches for heat transfer calculations. SAE Technical Paper, No. 790825, 1979
29. G. Vidyasagar Reddy, N. Govindha Rasu, T. Hari Prasad, Investigation on yttria stabilized zirconia coated Piston crown using different biodiesels. *Proc. Indian Natl. Sci. Acad.* (2019). <https://doi.org/10.16943/ptinsa/2019/49645>
30. D.V. Kumar, P.R. Kumar, M.S. Kumari, Prediction of performance and emissions of a biodiesel-fueled lanthanum–zirconate coated direct injection diesel engine using artificial neural networks. *Proc. Eng.* **64**, 993–1002 (2013)
31. R.L. Krupakaran, T. Hariprasad, A. Gopalakrishna, Impact of various blends of *Mimusops elengi* methyl esters on performance and emission characteristics of a diesel engine. *Int. J. Green Energy* **15**(7), 415–426 (2018)
32. M. Mohamed Mustafa, S.P. Sivapirakasam, M. Udayakumar, Comparative studies on fly ash-coated low heat rejection diesel engine on performance and emission characteristics fueled by rice bran and Pongamia methyl ester and their blend with diesel. *Energy* **36**, 2343–2351 (2011)
33. K. Rajan, K.R.S. Kumar, Combustion and emission characteristics of a biodiesel fuelled diesel engine with the effect of thermal barrier coated internal jet piston, in *International Conference on Sustainable Energy Intelligent Systems, 2011 (SEISCON 2011)*, pp. 184–189
34. H. Hazar, Effects of biodiesel on a low heat loss diesel engine. *Renew. Energy* **34**, 1533–1537 (2009)
35. I. Taymaz, A. Mimaroglu, E. Avci, V. Ucar, M. Gur, Comparison of thermal stresses developed in Al₂O₃-SG, ZrO₂-(12% SiCAl) and ZrO₂-SG thermal barrier coating systems with NiAl, NiCrAlY and NiCoCrAlY interlayer materials subjected to thermal loading. *Surf. Coat. Technol.* **116–119**, 690–693 (1999)
36. O.M.I. Nwafor, G. Rice, A.L. Ogabinnu, Effect of advance injection timing on the performance of rape seed oil in diesel engines. *J. Renew. Energy* **21**, 433–444 (2008)
37. M. Karabektas, The effects of turbocharger on the performance and exhaust emissions of a diesel engine fuelled with biodiesel. *Renew. Energy* **34**(4), 989–993 (2009)
38. M. Azadi, M. Baloo, G.H. Farrahi, S.M. Mirsalim, A review of thermal barrier coating effects on diesel engine performance and components lifetime. *Int. J. Autom. Eng.* **3**(10), 305–317 (2013)

Publisher's Note Springer Nature remains neutral with regard to jurisdictional claims in published maps and institutional affiliations.